Spin-polarized transport in graphene nanoribbon superlattices*

Yu Xin-Xin(余欣欣), Xie Yue-E(谢月娥),
OuYang Tao(欧阳滔), and Chen Yuan-Ping(陈元平)†

Institute of Physics and Laboratory for Quantum Engineering and Micro-Nano Energy Technology, Xiangtan University, Xiangtan 411105*, China*

(Received 8 March 2012; revised manuscript received 4 May 2012)

By the Green's function method, we investigate spin transport properties of a zigzag graphene nanoribbon superlattice (ZGNS) under a ferromagnetic insulator and edge effect. The exchange splitting induced by the ferromagnetic insulator eliminates the spin degeneracy, which leads to spin-polarized transport in structure. Spin-dependent minibands and minigaps are exhibited in the conductance profile near the Fermi energy. The location and width of the miniband are associated with the geometry of the ZGNS. In the optimal structure, the spin-up and spin-down minibands can be separated completely near the Fermi energy. Therefore, a wide, perfect spin polarization with clear stepwise pattern is observed, i.e., the perfect spin-polarized transport can be tuned from spin up to spin down by varying the electron energy.

Keywords: spintronics, superlattices, zigzag graphene nanoribbons

PACS: 72.80.Vp, 72.25.–b, 85.75.–d **DOI:** 10.1088/1674-1056/21/10/107202

1. Introduction

Graphene nanoribbons (GNRs) are regarded as promising candidates for spintronic devices due to their high carrier mobility,[1−4] low spin–orbit interaction,[5−7] and long spin-relaxation time.[8] Between the two typical edged GNRs, i.e., zigzag GNRs (ZGNRs) and armchair GNRs (AGNRs), ZGNRs have attracted more attention in the field of spintronic applications such as spin filters, because of their unique spin-polarized edge states.[9−11] However, perfect ZGNRs cannot generate spin polarization due to the spin degeneracy of the edge states. In order to obtain spin-polarized current, the spin degeneracy should be broken. A number of approaches are used to create spin-polarized current in the ZGNR by tuning the edge states, such as edge defect,[12−14] adsorption,[15,16] mechanical strain,[17] substrate,[18] and electric field.[19−21] However the spin polarizations produced by these approaches are achieved only near the Dirac point and the spin-polarized current is relatively small, which may restrict the possible applications of graphene-based devices in spintronics. Consequently, it is desirable to find a new approach to achieving large spin polarization and also large spin current in the ZGNRs.

Recently, utilizing graphene-based magnetic superlattices[22−24] to enhance spin polarization became very attractive in spintronic applications. Niu *et al.*[22] in their pioneering work have studied spin transport in a magnetic graphene superlattice, which can be realized by putting a series of ferromagnetic insulator[25−28] bars on the top of a graphene sheet. It is found that the spin polarization greatly increases with the periodic number of the superlattice increasing. However, the spin conductance still cannot be absolutely separated and the maximum of spin polarization is just about 80%. To further achieve a perfect spin polarization, our group[23] has studied spin transport properties of Fe atomic chain adsorbed on the ZGNRs. This quasi-magnetic graphene superlattice provides a wide range of complete spin polarization. These studies indicate that the graphene-based magnetic superlattices can produce remarkable spin polarization properties.

In the present paper, we propose a zigzag

*Project supported by the National Natural Science Foundation of China (Grant Nos. 51006086, 11074213, and 51176161), the Open Fund Based on Innovation Platform of Hunan Colleges and Universities, China (Grant No. 09K034), and the Joint Funds of Hunan Provincial Natural Science Foundation, China (Grant No. 10JJ9001).

†Corresponding author. E-mail: chenyp@xtu.edu.cn

© 2012 Chinese Physical Society and IOP Publishing Ltd

graphene nanoribbon superlattice (ZGNS) as shown in Fig. 1. A ferromagnetic insulator is deposited on the top of the whole superlattice and the edge effect[29,30] is considered in the sidearm of the ZGNS. Compared with a graphene-based magnetic superlattice, this kind of graphene nanoribbon superlattice can be obtained more easily in experiment.[31−33] The spin transport properties of the ZGNS are studied by using the Green's function method. Firstly, we calculate the spin conductance of the ZGNS with the increase of periodic number in the absence of exchange splitting. It is found that the two spin-dependent conductance profiles coincide with each other, and the minibands and minigaps are formed near the Fermi energy. As the exchange splitting is applied to the ZGNS, the spin degeneracy is broken and the spin-polarized transport is produced. The two spin-dependent conductance profiles shift toward the opposite directions, while some parts of the two minibands of different spin directions still overlap each other. Then the effects of geometry of the ZGNS on the spin-dependent miniband and minigap are discussed. It is shown that by choosing the optimized geometry parameters, the miniband of spin-up and that of spin-down can be separated completely near the Fermi energy. Therefore, a wide high tunable spin current with perfect spin polarization is realized. The results indicate that the ZGNS can serve as a spin filter.

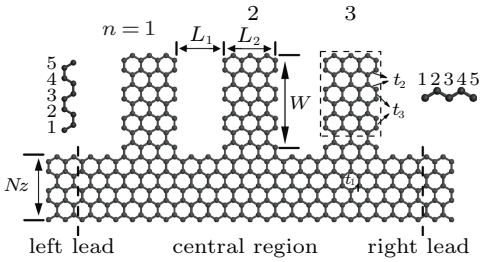


Fig. 1. Schematic view of the ZGNS with three stubs, where a finite central region is connected to two (left and right) semi-infinite leads with width Nz. The basic cell consists of a constriction with length L_1 and width Nz, connected to a stub of length L_2 and width $(Nz + W)$. n represents the periodic number of the superlattice. The left (right) inset represents the definition of width (length) of the system. The dashed frame denotes the sidearm of the ZGNS. A ferromagnetic insulator is deposited on the top of the whole superlattice.

2. Model and method

The geometry of a ZGNS is shown in Fig. 1. The system can be divided into three regions: left lead, central region, and right lead. The semi-infinite left and right leads each have a perfect periodicity along the ribbon axis with uniform width Nz. The finite central region is composed of constrictions with size $Nz \times L_1$ and stubs with size $(Nz + W) \times L_2$. Let n represent the periodic number of the superlattice. Figure 1 shows the case with $n = 3$, $Nz = 5$, $L_1 = 5$, $W = 7$, and $L_2 = 7$.

A ferromagnetic insulator is deposited on the top of the whole superlattice and induces an exchange splitting.[25,26] To describe the spin transport properties of the ZGNS, one uses the tight-binding Hamiltonian,[30,34,35]

$$H(M) = \sum_{i,s} (\varepsilon_i - \sigma M) c_{is}^{\dagger} c_{is} - t_{ij} \sum_{\langle ij \rangle, s} \left(c_{is}^{\dagger} c_{js} + \text{H.c.} \right), \quad (1)$$

where $c_{is}^{\dagger}$ and c_{is} are the creation and annihilation operators for an electron with spin s ($s = \uparrow, \downarrow$) on site i, respectively; $\varepsilon_i (= 0)$ is the on-site energy; M is the exchange splitting induced by the ferromagnetic insulator; $\sigma = \pm 1$ describe the up/down spin states; t_{ij} is the nearest-neighbour hopping energy. It is known that the edge effect has drastic influence on the electronic structure of AGNR, while the edge effect on ZGNR electronic structure is relatively weak. Therefore, the edge effect is considered only in the sidearm of the ZGNS (see the dashed frame in Fig. 1). In order to describe the edge effect of the ZGNS, for simplicity, we use t_1 to present the hopping energy between inner atoms while t_2 and t_3 to present the hopping energy between atoms on the armchair edge in the sidearm, where $t_1 = t = 2.7$ eV, $t_2 = 2.75$ eV, and $t_3 = 3.2$ eV.[29,30]

The lattice Green's function method is used to calculate spin transport properties[35] of the ZGNS. According to the Green's function scheme, the Green's function of the ZGNS can be expressed as[35]

$$\varsigma_r^{ss'}(E, M) = [EI - H_{\text{C}}(M) - \Sigma_{\text{L}}^{s}(E, M) - \Sigma_{\text{R}}^{s'}(E, M)]^{-1}, \quad (2)$$

where $H_{\text{C}}(M)$ is the Hamiltonian of the central region and $\Sigma_{\text{L(R)}}^{s(s')}(E, M)$ is the self-energy of the left (right) lead that can be calculated by the recursive Green's function method.[36,37] Once the total Green's function $\varsigma_r^{ss'}(E, M)$ is obtained, the spin conductance from the left lead with spin s to the right lead with spin s' and the local density of states (LDOS) of the system can be calculated by the following equations:[36,37]

$$G_{s's}(E, M) = \frac{e^2}{h} \text{Tr} \left[\Gamma_{\text{L}}^{s}(E, M) \varsigma_r^{ss'}(E, M) \Gamma_{\text{R}}^{s'}(E, M) \right.$$

$$\times \left[\varsigma_r^{ss'}(E,M)\right]^{\dagger}\Big], \tag{3}$$

$$\mathrm{LDOS} = -\mathrm{Im}\left[\varsigma_r^{ss'}(E,M)\right]/\pi, \tag{4}$$

where

$$\begin{aligned}&\Gamma_{\mathrm{L(R)}}^{s(s')}(E,M)\\ &= \mathrm{i}\left\{\Sigma_{\mathrm{L(R)}}^{s(s')}(E,M) - \left[\Sigma_{\mathrm{L(R)}}^{s(s')}(E,M)\right]^{\dagger}\right\}\end{aligned}$$

is the coupling function of the left (right) lead. With the spin conductances $G_{\uparrow\uparrow}$ and $G_{\downarrow\downarrow}$, the spin polarization P can be achieved by

$$P = (G_{\uparrow\uparrow} - G_{\downarrow\downarrow})/(G_{\uparrow\uparrow} + G_{\downarrow\downarrow}). \tag{5}$$

In the following, we consider the effect of exchange splitting on the spin conductance profile of the ZGNS. The Green's function of Hamiltonian $H_{\mathrm{C}}(M)$ is $\varsigma_r^{ss'}(E,M)$. When the exchange splitting increases to $M' = M + M_0$, the Green's function is transformed into $\varsigma_r^{ss'}(E, M+M_0)$ with Hamiltonian $H_{\mathrm{C}}(M+M_0)$. Due to the basic definition of Green's function $\varsigma(E,M') = [EI - H(M')]^{-1} = \varsigma(E+\sigma M, M_0)$, the self-energy $\Sigma_{\mathrm{L(R)}}^{s(s')}(E, M+M_0) = \Sigma_{\mathrm{L(R)}}^{s(s')}(E+\sigma M, M_0)$. Thus the Green's function $\varsigma_r^{ss'}(E, M+M_0)$ can be rewritten as

$$\begin{aligned}&\varsigma_r^{ss'}(E, M+M_0)\\ &= [(E+\sigma M)I - H_{\mathrm{C}}(M_0)\\ &\quad - \Sigma_{\mathrm{L}}^{s}(E+\sigma M, M_0) - \Sigma_{\mathrm{R}}^{s'}(E+\sigma M, M_0)]^{-1}.\end{aligned}$$

Therefore the Green's function and the coupling function of the ZGNS satisfy the following relations

$$\varsigma_r^{ss'}(E, M+M_0) = \varsigma_r^{ss'}(E+\sigma M, M_0), \tag{6}$$

$$\Gamma_{\mathrm{L(R)}}^{s(s')}(E, M+M_0) = \Gamma_{\mathrm{L(R)}}^{s(s')}(E+\sigma M, M_0). \tag{7}$$

These equations imply that

$$G_{\sigma_{\mathrm{R}}\sigma_{\mathrm{L}}}(E, M+M_0) = G_{\sigma_{\mathrm{R}}\sigma_{\mathrm{L}}}(E+\sigma M, M_0), \tag{8}$$

i.e., $G_{\uparrow\uparrow}(E, M+M_0) = G_{\uparrow\uparrow}(E+M, M_0)$ and $G_{\downarrow\downarrow}(E, M+M_0) = G_{\downarrow\downarrow}(E-M, M_0)$. As we set $M_0 = 0$, the above two equations can be simplified as

$$G_{\uparrow\uparrow}(E, M) = G_{\uparrow\uparrow}(E+M, 0), \tag{9}$$

$$G_{\downarrow\downarrow}(E, M) = G_{\downarrow\downarrow}(E-M, 0). \tag{10}$$

From Eqs. (9) and (10), we can conclude that the two spin-dependent conductance profiles just shift toward each other with their primary quality under the effect of exchange splitting M and the total translational distance of the two spin-dependent conductance profiles is $2M$.

In our calculation, energy E and exchange splitting M are measured in the units of the hopping energy t.

3. Results and discussion

In Fig. 2 we show the spin conductances of the ZGNS with different values of periodic number n at $M = 0$. Due to the absence of exchange splitting, the spin-up (solid line) and spin-down (dashed line) conductance coincide with each other. As $n = 1$ (the structure consists of one stub and two constrictions), it can be seen from Fig. 2(a) that there are two conductance antiresonant dips ($E = \pm 0.159\ t$) appearing symmetrically on the two sides of the Fermi energy ($E = 0$). These dips are caused by the quasi-bound states whose LDOS is displayed in the inset of Fig. 2(a). The electrons in the states are intensively confined in the stub. With the increase of periodic number n, the antiresonant dips develop into minigaps (see Figs. 2(b) and 2(c)). Meanwhile, it can be found that the conductance around $E = 0$ gradually drops and subsequently turns into an energy bandgap. As a result, the minibands and minigaps are formed near the Fermi energy. The minibands (minigaps) closest to the Fermi energy are called the first minibands (minigaps). The electrons in the minibands can pass

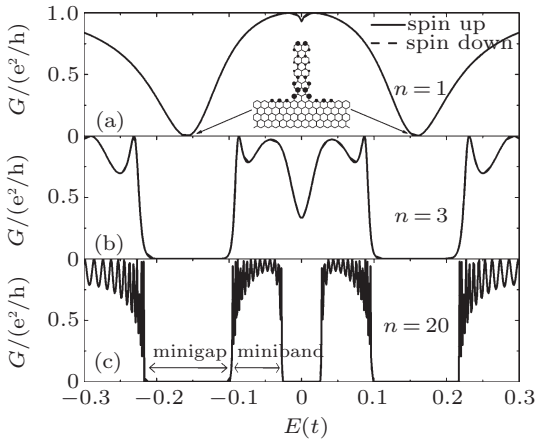


Fig. 2. Spin conductances of the ZGNS versus electron energy E for different values of periodic number n without exchange splitting: $n = 1$ (a), 3 (b), and 20 (c). Inset of panel (a) shows the spatial-resolved LDOS of quasi-bound state corresponding to the two conductance antiresonant dips at $E = \pm 0.159\ t$. The other parameters are chosen as follows: $Nz = 5$, $L_1 = 5$, $W = 9$, $L_2 = 5$, and $M = 0$.

through the superlattice with big probabilities while those in the minigaps undergo filtration (prohibited).

As exchange splitting M is applied to the ZGNS, the spin conductance versus electron energy E is shown in Fig. 3(a). Comparing with Fig. 2(c), one can find that the degeneracy of the two spin-dependent conductance is eliminated by the exchange splitting. The two conductance profiles shift toward the opposite directions, and the total translational distance should be $2M$ according to Eqs. (9) and (10). Meanwhile, one can also find that some parts of the two minibands of different spin directions still overlap each other. The nonoverlapping regions display perfect spin polarizations while the spin polarizations in the overlapping regions are very small as shown in Fig. 3(b). Therefore, in order to achieve perfect spin polarizations for all electrons in the minibands, the minibands of different spin directions should be separated completely. Here we consider only the minibands near the Fermi energy. When the bandgap $\Delta_0 \geq 0$ and the overlapping region $\Delta_1 = 0$, the first miniband of spin up and that of spin down will just be separated completely. In this case, the spin-up or spin-down minigap ξ_0 should be greater than ξ_1 of the first miniband, i.e., $\xi_0 > \xi_1$, and also the first spin-up or spin-down miniband should satisfy $\xi_2 > \xi_1$. Obviously, in Fig. 3(a), the first minibands of different spin directions cannot be separated completely no matter how strong the exchange splitting is, owing to the fact that ξ_0 is smaller and ξ_2 is larger than ξ_1. To obtain these conditions, one should adjust the geometry of the ZGNS.

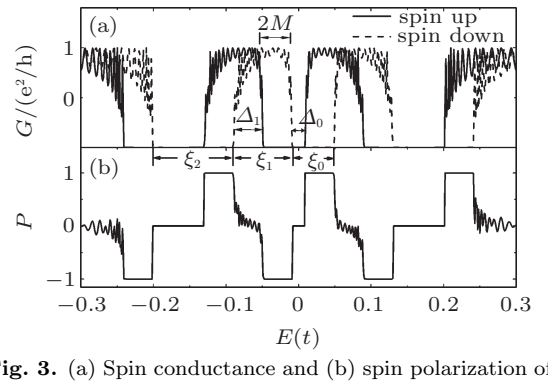


Fig. 3. (a) Spin conductance and (b) spin polarization of the ZGNS versus electron energy E. The symbols Δ_0 and Δ_1 in panel (a) denote, respectively, the bandgap and the overlapping region, while the symbols ξ_0 and ξ_2 represent the different spin-dependent minigaps , and ξ_1 denotes the spin-dependent miniband. The parameters are chosen as follows: $n = 20$, $Nz = 5$, $L_1 = 5$, $W = 9$, $L_2 = 5$, and $M = 0.02\ t$.

In Fig. 4, the effects of geometry of the ZGNS on the spin-dependent miniband ξ_1 and minigaps ξ_0 and ξ_2 are discussed. Figure 4(a) shows the effect of constriction length L_1, while figure 4(b) shows the effect of stub width W. One can find that the spin-dependent minigaps ξ_0 and ξ_2 both increase as length L_1 decreases, while miniband ξ_1 slightly decreases with length L_1 increasing (see Fig. 4(a)). As $L_1 < 4$, two conditions $\xi_0 > \xi_1$ and $\xi_2 > \xi_1$ are achieved. On the other hand, one can find from Fig. 4(b) that ξ_1 decreases with the increase of width W, while ξ_0 and ξ_2 are insensitive to the variation of width W. The decrease of ξ_1 originates from the fact that the energies of the quasi-bound states at $E = \pm 0.159\ t$ in Fig. 2(a) shift toward the Fermi energy as the width W increases.[38] Figure 4(b) indicates that the width W of the stub should be large enough so as to satisfy $\xi_0 > \xi_1$ and $\xi_2 > \xi_1$.

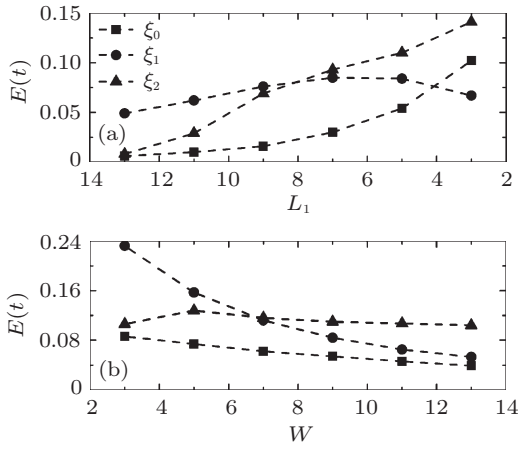


Fig. 4. (a) Variations of ξ_0, ξ_1, and ξ_2 each as a function of length L_1, where the other parameters are chosen as follows: $n = 20$, $Nz = 5$, $W = 9$, $L_2 = 5$, and $M = 0.02\ t$. (b) Variations of ξ_0, ξ_1, and ξ_2 each as a function of width W, where the other parameters are chosen as follows: $n = 20$, $Nz = 5$, $L_1 = 5$, $L_2 = 5$, and $M = 0.02\ t$.

In light of the above discussion, we calculate the spin conductance and spin polarization of the ZGNS with length $L_1 = 3$ and width $W = 11$, and the results are shown in Fig. 5. It can be seen from Fig. 5(a) that the minibands of different spin directions are separated completely near the Fermi energy. Correspondingly, the spin polarization exhibits clear stepwise variation from 100% to –100% in a broad energy window (see Fig. 5(b)). In this case the spin is completely polarized in most of the energy range and the spin-polarization orientation can be controlled effectively by tuning electron energy E.

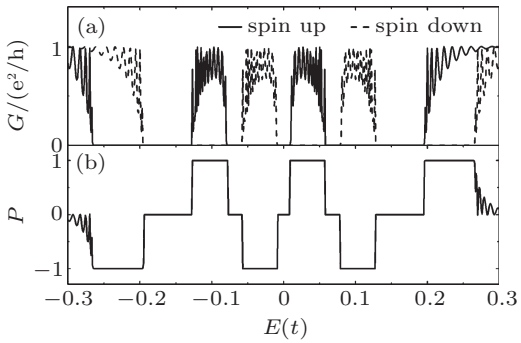


Fig. 5. (a) Spin conductance and (b) spin polarization of the ZGNS versus electron energy E. The parameters are chosen as follows: $n = 20$, $Nz = 5$, $L_1 = 3$, $W = 11$, $L_2 = 5$, and $M = 0.035\ t$.

4. Conclusions

In this paper, using the Green's function method, we study the spin-polarized transport properties of a ZGNS with a ferromagnetic insulator deposited on the top. And the edge effect is considered in the sidearm of the ZGNS. The exchange splitting M induced by the ferromagnetic insulator eliminates the spin degeneracy and leads to spin-polarized transport in the superlattice. The two spin-dependent conductance profiles shift toward the opposite directions, and the total translational distance is $2M$. Meanwhile, minibands and minigaps of different spin directions are formed in the conductance profile near the Fermi energy. The location and width of the miniband are associated with the geometry of the ZGNS. When the constriction length is small enough and the stub width is large enough, the miniband of spin-up and that of spin-down can be separated completely near the Fermi energy. In this case, the spin polarization of the ZGNS can be tuned from 100% to –100%, i.e., the perfect spin-polarized transport can be changed from spin up to spin down by changing the electron energy. The results indicate that the ZGNS can be used as a spin filter.

References

[1] Li X, Wang H, Zhang L, Lee S and Dai H 2008 *Science* **319** 1229

[2] Wang X, Ouyang Y, Li X, Wang H, Guo J and Dai H 2008 *Phys. Rev. Lett.* **100** 206803

[3] Lin X, Wang H L, Pan H and Xu H Z 2011 *Chin. Phys.* B **20** 047302

[4] Xu X G, Zhang C, Xu G J and Cao J C 2011 *Chin. Phys.* B **20** 027201

[5] Huertas-Hernando D, Guinea F and Brataas A 2006 *Phys. Rev.* B **74** 155426

[6] Min H, Hill J E, Sinitsyn N A, Sahu B R, Kleinman L and MacDonald A H 2006 *Phys. Rev.* B **74** 165310

[7] Yao Y, Ye F, Qi X L, Zhang S C and Fang Z 2007 *Phys. Rev.* B **75** 041401

[8] Tombros N, Jozsa C, Popinciuc M, Jonkman H T and Wees B J 2007 *Nature* **448** 571

[9] Kobayashi Y, Fukui K, Enoki T, Kusakabe K and Kaburagi Y 2005 *Phys. Rev.* B **71** 193406

[10] Niimi Y, Matsui T, Kambara H, Tagami K, Tsukada M and Fukuyama H 2006 *Phys. Rev.* B **73** 085421

[11] Wakabayashi K, Fujita M, Ajiki H and Sigrist M 1999 *Phys. Rev.* B **59** 8271

[12] Wimmer M, Adagideli İ, Berber S, Tománek D and Richter K 2008 *Phys. Rev. Lett.* **100** 177207

[13] Kumazaki H and Hirashima D S 2009 *J. Phys. Soc. Jpn.* **78** 094701

[14] Hancock Y, Uppstu A, Saloriutta K, Harju A and Puska M J 2010 *Phys. Rev.* B **81** 245402

[15] Cocchi C, Prezzi D, Calzolari A and Molinari E 2010 *J. Chem. Phys.* **133** 124703

[16] Rigo V A, Martins T B, Silva A J R, Fazzio A and Miwa R H 2009 *Phys. Rev.* B **79** 075435

[17] Guo Y F and Guo W L 2012 *J. Appl. Phys.* **111** 074317

[18] Zhang Z H, Chen C F and Guo W L 2009 *Phys. Rev. Lett.* **103** 187204

[19] Guo Y F, Guo W L and Chen C F 2010 *J. Phys. Chem.* C **114** 13098

[20] Son Y W, Cohen M L and Louie S G 2006 *Nature* **444** 347

[21] Kan E J, Li Z, Yang J and Hou J G 2007 *Appl. Phys. Lett.* **91** 243116

[22] Niu Z P, Li F X, Wang B G, Sheng L and Xing D Y 2008 *Eur. Phys. J.* B **66** 245

[23] Zhang Z L, Chen Y P, Xie Y E, Zhang M and Zhong J X 2011 *J. Phys.* D: *Appl. Phys.* **44** 215403

[24] Ke Q R, Lü H F, Chen X D and Zu X T 2011 *Solid State Commun.* **151** 1131

[25] Haugen H, Huertas-Hernando D and Brataas A 2008 *Phys. Rev.* B **77** 115406

[26] Huard B, Sulpizio J A, Stander N, Todd K, Yang B and Goldhaber-Gordon D 2007 *Phys. Rev. Lett.* **98** 236803

[27] Zhao H, Zhang X W, Cai T, Sang T, Liu X C and Liu F 2012 *Chin. Phys.* B **21** 017305

[28] Tian H Y and Wang J 2012 *Chin. Phys.* B **21** 017203

[29] Son Y W, Cohen M L and Louie S G 2006 *Phys. Rev. Lett.* **97** 216803

[30] Sun L, Li Q X, Ren H, Su H B, Shi Q W and Yang J L 2008 *J. Chem. Phys.* **129** 074704

[31] Novoselov K S, Geim A K, Morozov S V, Jiang D, Zhang Y, Dubonos S V, Grigorieva I V and Firsov A A 2004 *Science* **306** 666

[32] Novoselov K S, Geim A K, Morozov S V, Jiang D, Katsnelson M I, Grigorieva I V, Dubonos S V and Firsov A A 2005 *Nature* **438** 197

[33] Ci L, Song L, Jariwala D, ElÃ-as A L, Gao W, Terrones M and Ajayan P M 2009 *Adv. Mater.* **21** 4487

[34] Nguyen V H, Nam Do V, Bournel A, Nguyen V L and Dollfus P 2009 *J. Appl. Phys.* **106** 053710

[35] Sun Q F and Xie X C 2010 *Phys. Rev. Lett.* **104** 066805

[36] Chen Y P, Xie Y E, Sun L Z and Zhong J X 2008 *Appl. Phys. Lett.* **93** 092104

[37] Chen Y P, Xie Y E and Yan X H 2008 *J. Appl. Phys.* **103** 063711

[38] Li H, Chen Y P, Xie Y E and Zhong J X 2011 *J. Appl. Phys.* **110** 033701